Journal of Physics: Conference Series **219** (2010) 032015 doi:10.1088/1742-6596/219/3/032015

Ring Recognition and Electron Identification in the RICH detector of the CBM Experiment at FAIR

S. Lebedev [1,2], C. Höhne [1], G. Ososkov[2] for the CBM Collaboration

[1] GSI Helmholtzzentrum für Schwerionenforschung GmbH, 64291 Darmstadt, Germany
[2] Joint Institute for Nuclear Research, Laboratory of Information Technologies, 141980 Dubna, Russia

E-mail: S.Lebedev@gsi.de

Abstract. The Compressed Baryonic Matter (CBM) experiment at the future FAIR facility at Darmstadt will measure dileptons emitted from the hot and dense phase in heavy-ion collisions. In case of an electron measurement, a high purity of identified electrons is required in order to suppress the background. Electron identification in CBM will be performed by a Ring Imaging Cherenkov (RICH) detector and Transition Radiation Detectors (TRD).

In this contribution we will present algorithms and software which have been developed for electron identification in CBM. Efficient and fast ring recognition in the RICH detector is based on the Hough Transform method which has been accelerated considerably compared to a standard implementation. Ring quality selection is done using an Artificial Neural Network which also has been used for electron identification. Due to optical distortions ellipse fitting and radius correction routines are used for improved ring radius resolution.

These methods allow for a high purity and efficiency of reconstructed electron rings. For momenta above 2 GeV/c the ring reconstruction efficiency for electrons embedded in central Au+Au collisions at 25 AGeV beam energy is 95% resulting in an electron identification efficiency of 90% at a pion suppression factor of 500. Including information from the TRD a pion suppression of 10^4 is reached at 80% efficiency.

The developed algorithm is very robust to a high ring density environment. Current work focusses on detector layout studies in order to optimize the detector setup while keeping a high performance. All developed algorithms were tested on large statistics of simulated events and are included into the CBM software framework for common use.

1. Introduction

The Compressed Baryonic Matter (CBM) experiment [1] is designed to investigate nucleus-nucleus collisions from 10-45 AGeV beam energy at the future international FAIR project. The objective of heavy-ion collision experiments is to explore the QCD phase diagram. CBM will investigate the phase diagram at high baryon densities but moderate temperatures. In this intermediate range of the phase diagram, structures such as the first order phase transition between hadronic and partonic matter and the critical endpoint are of special interest. The CBM experiment aims at discovering these structures by systematic and comprehensive investigations of hadron and lepton production in heavy-ion collisions. Special focus is set on rare probes not yet been measured at these energies. Charm production is explored at threshold and the propagation of charmed hadrons is expected to be sensitive to the matter created in these collisions. Vectormesons decaying into dileptons are an ideal probe of the hot and dense fireball

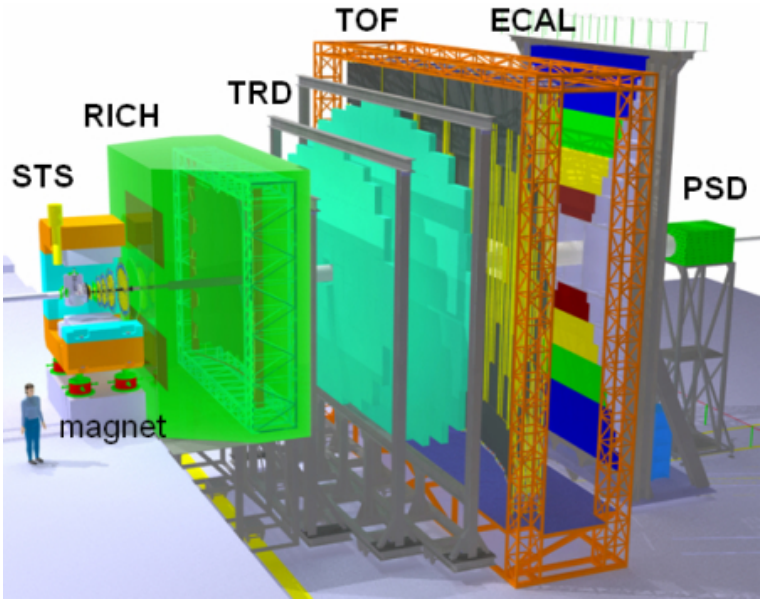

Figure 1. Layout of the CBM experiment.

as the leptons leave the interaction zone undistorted. In this contribution, the current status of electron identification needed for the reconstruction of J/ψ and ψ' mesons as well as for low mass vectormesons (ρ, ω, ϕ) is presented.

The experimental task is to identify both hadrons and leptons and to detect rare probes in the environment of heavy-ion collisions. The challenge is to select such rare events in nucleus-nucleus collisions with charged particle multiplicities of about 1000 per central event at reaction rates of up to 10 MHz. Such measurements require fast and radiation hard detectors, fast and self-triggered read-out electronics, a high-speed data acquisition system, online event selection based on track reconstruction, and even fast offline tracking and event reconstruction routines.

The proposed detector system is schematically shown in Fig 1. The core of the CBM detector is a Silicon Tracking System (STS) in a magnetic dipole field. The STS provides track and vertex reconstruction and momentum determination. Detectors for particle identification will be placed behind the magnet: a Ring Imaging Cherenkov (RICH) detector together with Transition Radiation Detectors (TRD) for electron identification and a time-of-flight (TOF) wall for hadron identification. The setup will be completed by an Electromagnetic CALorimeter (ECAL) for the measurement of direct photons in selected regions of phase space and a Projectile Spectator Detector (PSD) for the determination of collision centrality and of the reaction plane.

2. The RICH detector

The RICH detector in CBM [2] will serve for electron identification from lowest momenta up to 10 GeV/c needed for the study of the dielectronic decay channel of vector mesons. The required pion suppression for RICH is of the order of 500-1000 and together with TRD of the order of 10^4.

Currently two different RICH designs are under discussion [2]. Both designs provide about 22 hits/ring but differ in length due to different choices of radiator gas. The larger option would be run with nitrogen as radiator, has a radiator length of 2.25 m and a resulting ring radius for electrons of about 6 cm. In the smaller option CO_2 would be used as radiator gas and the ring radius of electrons would be about 5 cm due to a smaller mirror curvature and reduced radiator

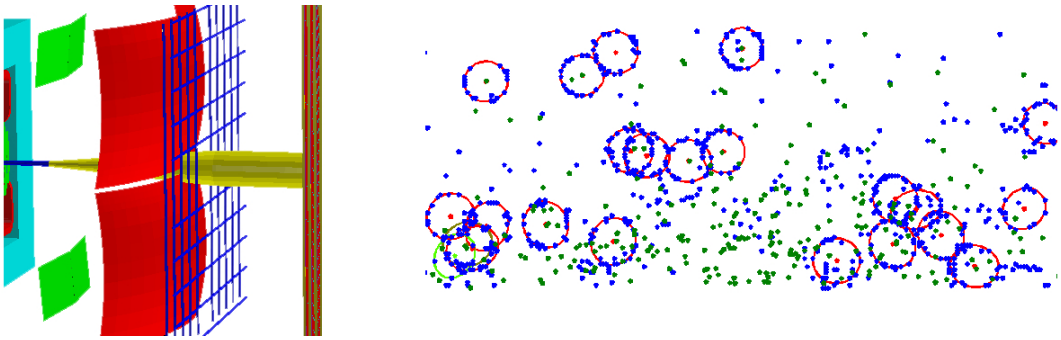

Figure 2. Left: Sketch of the RICH setup as used in simulations (outer gas box omitted). Right: Part of one typical event in the smaller CO_2-RICH: RICH hits (blue), found RICH rings (red), track projections form the STS (green).

length of 1.5 m. As the photodetector can only approximately be placed into the focal plane, rings are typically distorted to ellipses with about 10% difference in the length of major and minor half axis. As photodetector MAPMTs from Hamamatsu (H8500-03) are implemented: 200k channels for the N_2-RICH and 55k for the CO_2-RICH. The dimensions of the sensitive pads for H8500-03 are appr. 0.6x0.6 cm^2, which is of the order of 10% of the ring radius. The ring and hit density on the photodetector plane is non-uniform and depends on the position on the photodetector. The inner part which is closer to the beam pipe has the highest ring densities. For the smaller RICH setup the ring density is higher than for the larger one, which poses an additional challenge for the ring recognition. Fig. 2 illustrates the layout of the RICH detector in the GEANT simulations of CBM and a typical event display for a part of the photodetector plane including track projections which are later used in the analysis.

3. Event reconstruction in the CBM RICH detector

The event reconstruction in the RICH detector includes several steps. First, reconstructed STS tracks are extrapolated to the mirrors. These tracks are then reflected onto the photodetector plane providing track positions in this plane. Rings are searched for as described below, finally grouping certain hits to a ring. A further ring fit (either circle or ellipse fit) provides more precise values of its radius and center. The last step is to match the found rings with the extrapolated tracks.

3.1. Ring recognition algorithm

The main challenge of the ring recognition in the CBM RICH detector results from the large multiplicity in heavy-ion collisions. About 1000 particles are produced in central Au+Au collisions at CBM energies. This high charged particles multiplicity leads to a high ring density in the RICH detector (appr. 100 rings per event). Most measured electrons are electrons produced in the STS detector or magnet yoke. This material budget significantly increases the ring density in the RICH detector and causes many overlapping rings. The resolution of the Cherenkov angle, i.e. ring resolution is determined to approximately similiar magnitude by multiple scatering, distortions from the residual magnetic field and detector granularity. As mentioned above, rings are slightly distorted to ellipses, because the flat photodetector can only be approximately placed in the focal plane.

The developed ring recognition algorithm is standalone, i.e the input data is only an array of RICH hits without information from other detectors. The algorithm consists of two steps. First, a local search of ring-candidates is performed. It is based on local selection of hits and

the Hough Transform (HT) [3, 4, 5]. The second step is a global search, in which mainly the quality of rings is determined using an artificial neural network (ANN). This step is used as filter: collecting information about all ring-candidates, the algorithm compares them and chooses only high quality rings, rejecting repeatedly found rings (clone rings) and wrongly found rings (fake rings).

3.1.1. Hough Transform for ring recognition The Hough Transform (HT) [3, 4, 5] is a standard method for curve recognition in digital images, e.g. for finding straight lines, circles or ellipses. Using the HT one tries to combine the points of interest to such predefined curve shapes. A set of curves on a 2D plane is specified by the parametric equation: $F(a_1, a_2, a_3, ..., a_n, x, y) = 0$, where F is some function, a_1, a_2,... are parameters of the set of curves, and x, y are the coordinates on the plane. The parameters of the curves form the space of parameters (or Hough space), each point in this space (specific set of parameters a_1, a_2,...) corresponds to a certain curve.

The equation $F(a, b, R, x, y) = (x - a)^2 + (y - b)^2 - R^2$ describes a set of circles. Any three points (a triplet) unambiguously determines a circle, i.e. the three parameters (a, b, R). Solving the system of equations yields the following values for the center coordinates and the radius:

$$a = \frac{1}{2}\frac{(x_2^2 - x_3^2 + y_2^2 - y_3^2)(y_1 - y_2) - (x_1^2 - x_2^2 + y_1^2 - y_2^2)(y_2 - y_3)}{(x_2 - x_3)(y_1 - y_2) - (x_1 - x_2)(y_2 - y_3)} \tag{1}$$

$$b = \frac{1}{2}\frac{(x_1^2 - x_2^2 + y_1^2 - y_2^2)(x_2 - x_3) - (x_2^2 - x_3^2 + y_2^2 - y_3^2)(x_1 - x_2)}{(x_2 - x_3)(y_1 - y_2) - (x_1 - x_2)(y_2 - y_3)} \tag{2}$$

$$R = \sqrt{(x_1 - a)^2 + (y_1 - b)^2} \tag{3}$$

where (x_1, y_1), (x_2, y_2), (x_3, y_3) are the coordinates of the 1st, 2nd, 3rd point, respectively.

Instead of combining all possible hit triplets in the photodetector plane, we use the fact that the RICH rings have a maximum radius R_{max} because of the limiting Cherenkov angle. Hit triplets are only combined within this distance plus a safety margin, e.g. within $2R_{max} = D_{max}$. The recognition procedure then starts from the first hit in a hit array, which defines the preliminary position of the first ring. Then all hits are collected lying whithin the predefined region around the initial hit (see Fig. 3, left). This way, rings are only searched locally.

In the next step center and radius are calculated using equations (1), (2) and (3) from every triplet of selected hits. The calculated values are filled in the histograms of ring parameters. As a ring has three parameters one would need a 3D histogram. However this approach would need too much memory. Therefore, in our approach two independent histograms are used: a 2D histogram for ring centers (see Fig. 3, right) and a 1D histogram for the radii. Note that the 2D histogram is created only in a local area, thus it has small dimensions (here: 15 by 15 bins), this significantly reduces memory consumption and computational time. When the histograms are built, strong peaks in each histogram should correspond to the supposed positions of ring centers (2D histogram) and radii (1D histogram). If the peak is higher than a prescribed cut this ring-candidate is accepted and shifted to the ring-candidate array, otherwise rejected.

3.1.2. Ring quality calculation for fake ring rejection The above described local ring-candidate search algorithm finds not only correct rings, corresponding to Monte-Carlo rings in our simulation, but also wrong rings which are formed by random combinations of hits. Often this is a result of the high ring density and noise hits. A typical scenario of wrongly found rings (fake rings) is the assignment of hits from nearby rings forming an additional ring in between those rings.

In order to reliably reject these fake rings, a set of ring characteristics had to be selected which could be used for a quality estimation of found rings. These properties have to differ significantly

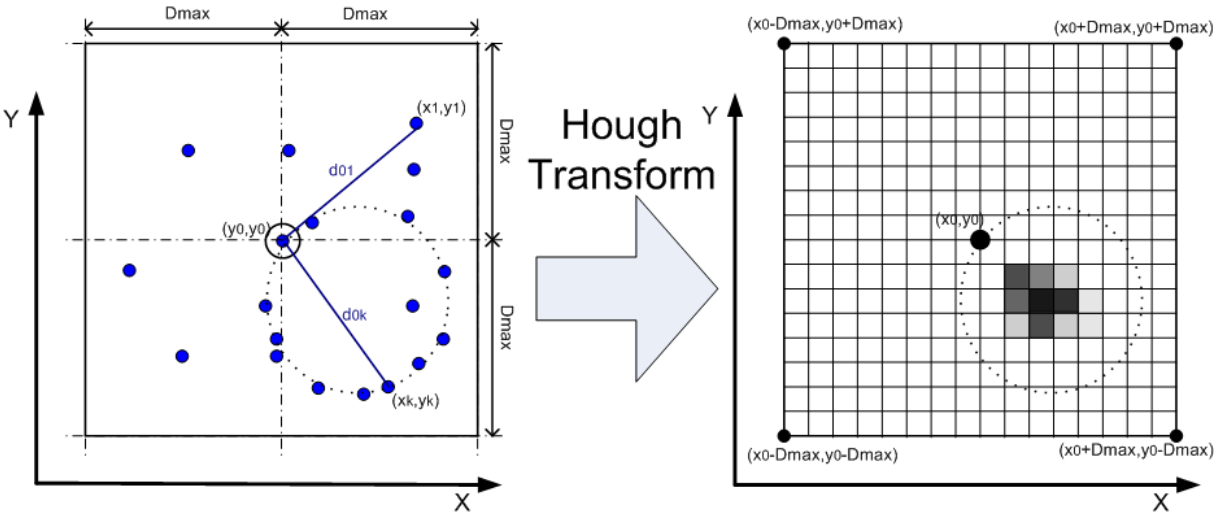

Figure 3. Preliminary search of the hit in the local area defined by the maximum ring radius plus a safety margin(left). Schematic view of the 2D histogram of ring centers (right). D_{max} is the maximum diameter of the ring, and (x_0, y_0) are the coordinates of the initial hit.

Figure 4. Illustration of the narrow corridor around the ring (left) and the angles between neighboring hits (right).

for wrongly and correctly found rings. After a statistical analysis nine parameters were selected: the number of hits per ring; the sum of the three biggest angles between neighboring hits in the ring (see Fig. 4, right); the number of hits in a small corridor around the ring (see Fig. 4, left); the position of the ring in the RICH detector; major and minor half axes of the fitted ellipse; χ^2 of the ellipse fitting; rotation angle of the ellipse vs. azimuthal angle.

An artificial neural network (ANN) was used for the ring quality calculation. The ANN derives the ring quality using the nine input parameters described above. Here the ANN implementation of the multilayer perceptron type from the ROOT package was used [8]. In our case, the ANN consists of nine input neurons corresponding to the nine parameters. Best results were obtained if the number of neurons in the hidden layer was twice as much as the neurons in the input layer. One output neuron is used. For the ANN training procedure 3000 wrongly found rings and 3000 correctly found rings were used, both extracted from simulations using Monte-Carlo methods. In the ANN training, the output value for fake rings was set to -1 and for correctly found rings to 1. For real events the output value of the ANN is not binary (see Fig. 5): values only concentrate around ± 1. Thus, as output of the ANN one gets some kind of ring quality measure or probability, whether a ring-candidate was correctly found or not.

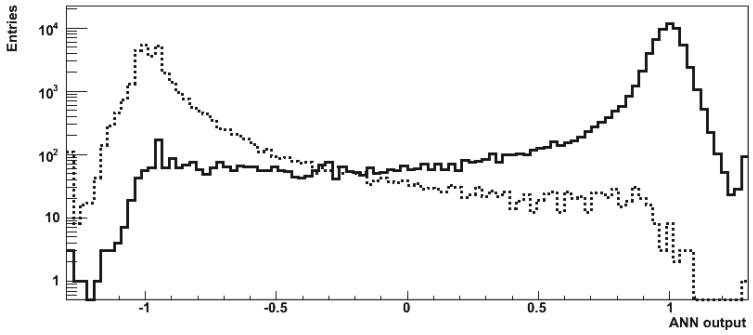

Figure 5. Distribution of the ANN output value from real events (Au+Au collisions at 25 AGeV beam energy, from UrQMD) after training for wrongly found rings (dashed line) and correctly found rings (solid line).

3.1.3. Global search algorithm The selection of good rings from the array of found ring-candidates is based on the ring quality which has been calculated by the ANN. With this information, the algorithm compares the ring quality choosing good rings and rejecting repeatedly found rings (clones) and wrongly found rings: first, the array of rings is sorted by the ring quality, thus starting with the highest quality rings. When filling the output ring array, the algorithm checks for shared hits with all other ring-candidates. If the ring shares more than 30% of its hits with better quality rings it is rejected.

3.2. Parameter Determination of the Rings

3.2.1. Circle fitting algorithm Because of its simplicity circle fitting is used in the ring recognition algorithm. The main requirement to this algorithm is a very high computational speed while keeping reasonable accuracy. We used the algorithm which is known as COP (Chernov-Ososkov-Pratt) [6]. In the COP algorithm the following functional is minimized:

$$\bar{M}(a,b,R) = \sum_{i=1}^{n} \left[\left((x_i - a)^2 + (y_i - b)^2 - R^2 \right)^2 / 4 * R^2 \right] \tag{4}$$

The COP algorithm is implemented such that the Newton method for nonlinear equations with one varible is used for the minimization of the functional (4). The algorithm is very robust to the initial parameters and converges for 3-4 iterations.

3.2.2. Ellipse fitting algorithm As described above, the rings in the CBM RICH detector have a slight elliptic shape, therefore an ellipse fitting method was implemented for more precise parameter determination.

An algorithm based on the Taubin method was implemented [7]. The general equation of ellipses described as conic sections is $P(x) = Ax^2 + Bxy + Cy^2 + Dx + Ey + F$. The functional which has to be minimized in the algorithm is constructed as the sum of all squared deviations of the measured points from the ellipse described by $P(x)$. The deviations were measured perpendicular to $P(x)$. Minimization parameters were A, B, C, D, E, F. To avoid non-linearity a Tailor expansion of the functional is used. This results in a very fast and direct algorithm, which is non-iterative and does not need starting parameters.

3.2.3. Radius correction Measured values of the major and minor axes of the ellipse depend on their position on the photodetector plane. The mean value of the major axes varies from 5.8

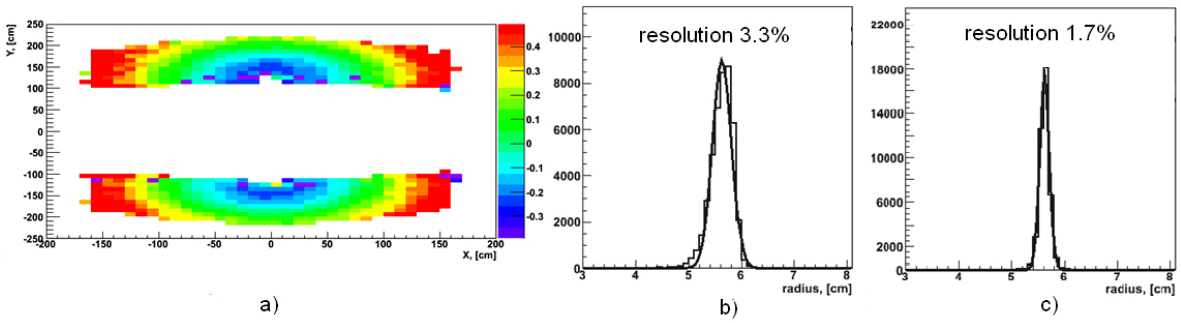

Figure 6. a) Correction map, colors show the difference (in cm) between the mean minor halfaxes value and minor halfaxes value in the certain area on the PMT plane. b) Distribution of the minor halfaxes before correction. c) Distribution of the minor halfaxes after correction.

cm in the outer part of the photodetector plane to 6.6 cm in the inner part, for the minor axes it varies from 5.2 cm to 5.9 cm. Therefore a radius (axes) correction algorithm was introduced for an improved radius resolution and thus pion suppression. The algorithm is based on a correction map, which has been obtained from large simulated statistics. Applying this correction improves the resolution by a factor of two (see Fig. 6).

3.3. Ring finding efficiency

In order to test the ring reconstruction algorithm, central Au+Au collisions at 25 AGeV beam energy were simulated with UrQMD [9]. Additional electrons at the primary vertex were embedded in these events in order to estimate their reconstruction efficiency. About 100 rings per event are seen in the RICH detector, mostly from secondary electrons. As mentioned above two different RICH designs are under discussion. In Fig. 7 results of the ring finding algorithm are shown for both designs. In both cases the ring finding efficiencies for electrons are larger than 90%. In the larger N_2-RICH efficiencies are as high as 95% while dropping by 2% for the smaller CO_2-RICH with higher ring densities. As the number of channels is reduced by 70% between the two designs these 2% losses are well tolerable. Overall, typically 4% of the approximately 100 found rings are fake rings and 2% clone rings.

The developed algorithm was tested with more than double the typical ring density in order to understand its robustness to extreme experimental situations. Even in this case where most of the rings start overlapping efficiencies drop by a few percent only. The algorithm is also stable to a reduction of hits/ring to 70%.

4. Electron identification in CBM

After reconstructing the rings in the RICH detector, these rings are matched to reconstructed tracks from the STS detector which were extrapolated to the RICH photodetector plane (see Fig. 2(right)). This matching is done on the basis of selecting the shortest possible distance between ring centers and extrapolated track positions. For correctly found and matched rings this distance peaks around 0.2 cm (see Fig. 8c). Applying a cut on the ring-track distance allows to reject false combinations. Such combinations are typically rings from secondary electrons which have not been reconstructed as tracks to track extrapolations from primary vertex pions. Here, a cut at 1 cm is used, the cut can be chosen momentum dependent for higher efficiencies at low momenta.

Electrons in the RICH detector are identified by a $\pm 3\sigma$ cut around the mean values of the minor and major halfaxis (see Fig. 8 a+b). This cut is done momentum independent as electrons

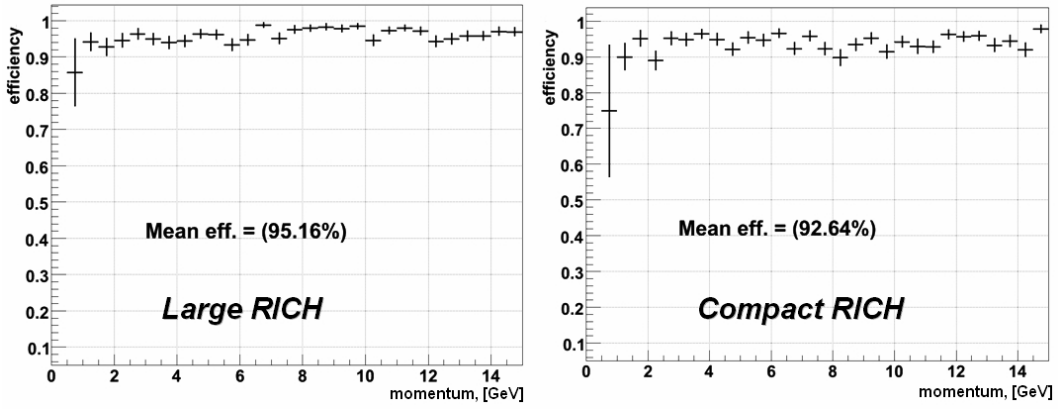

Figure 7. Ring finding efficiency for electrons in dependence on momentum for the larger N_2-RICH (left) and the smaller CO_2-RICH (right).

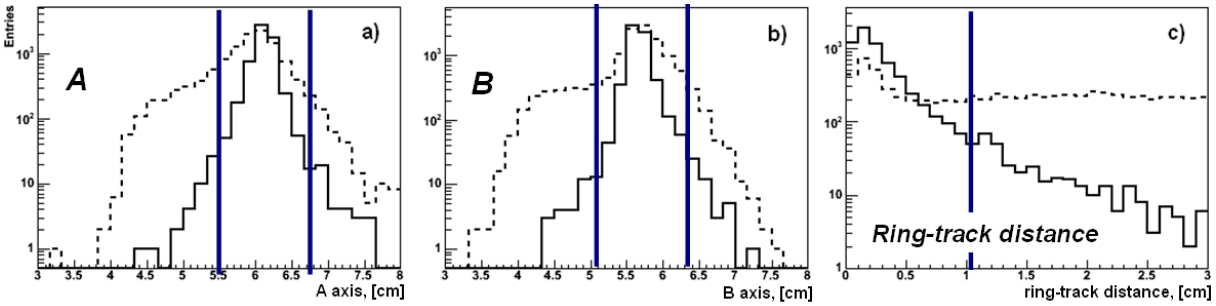

Figure 8. Momentum integrated distributions of the minor halfaxis (a), major halfaxis (b) and shortest ring-track distance (c). Distributions for pions are shown as dashed line, for electrons as solid line.

always show the maximum Cherenkov angle and because the ring resolution depends only little on momentum. The broad distributions seen for pion rings in Fig. 8 a+b results from the momentum dependence of their ring radius.

The RICH detector alone yields a pion suppression factor of 500 at an electron identification efficiency of 90%. In combination with the TRD detector a factor 10^4 is reached at 83% efficiency (see Fig. 9). Physics feasibility studies have shown that such a pion suppression factor is sufficient. In this case, the remaining background is dominated by physics sources [10].

5. Summary

A fast and efficient algorithm for ring recognition in the CBM RICH detector has been developed. The ring recognition is based on the Hough Transform method with a local selection of hits. An ellipse fitting algorithm has been implemented for precise estimation of ring parameters. A global ring search algorithm has been developed to select only good rings, while rejecting fake rings and clone rings. The time of the reconstruction of one event in RICH with typically more than 100 rings is from 50 ms to 300 ms on a Pentium4 2GHz. The variation of time depends on selected parameters in the ring reconstruction trading efficiency vs. speed. The algorithm has shown a very good performance in terms of ring finding efficiency and is robust towards a high ring multiplicity environment.

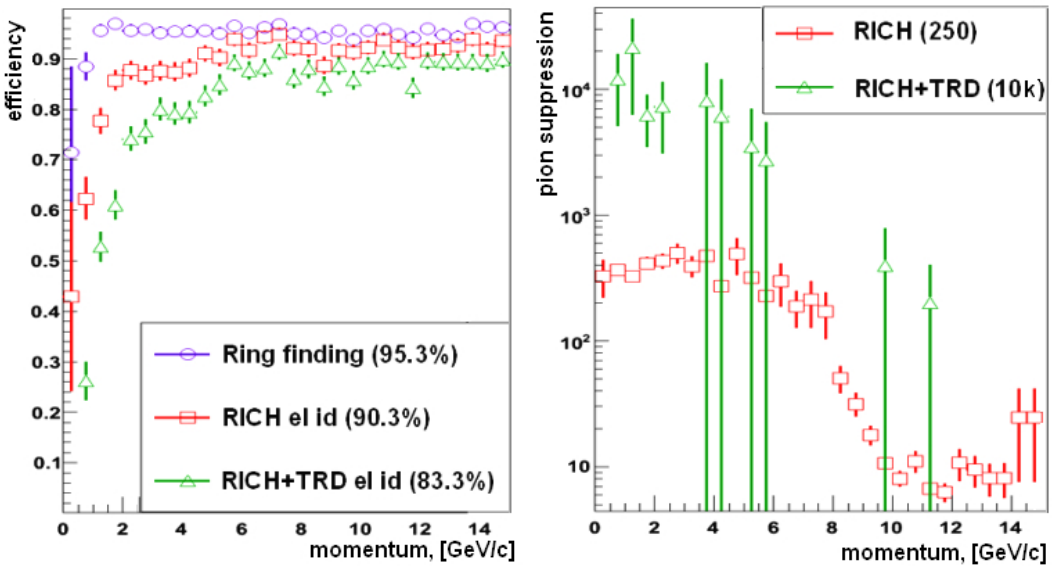

Figure 9. Electron identification efficiency (left) and pion suppression factor (right) for simulations of central Au+Au collisions at 25 *A*GeV beam energy (UrQMD).

6. References

[1] CBM Collaboration 2005 *Compressed Baryonic Matter Experiment. Technical Status Report.* GSI, Darmstadt
[2] C Höhne et al. 2008 *Nucl. Inst. and Meth. A* 595, 187
[3] P V C Hough 1962 A Method and Means for Recognizing Complex Patterns *US Patent* : 3, 069, 654
[4] J Radon Über die Bestimmung von Funktionen durch ihre Integralwerte längs gewisser Mannigfaltigkeiten. Ber. Ver. Sächs. Akad. Wiss. Leipzig, Math-Phys. Kl., 69, 1917 p. 262-277
[5] P Toft 1996 The Radon Transform. Theory and Implementation. Ph.D. Thesis. Technical University of Denmark
[6] N Chernov , G Ososkov 1984 *Comp. Phys. Comm.*, **33** p. 329-333
[7] N Chernov 2007 *J Math Im Vi*, 27 p. 231-239
[8] ROOT - An Object-Oriented Data Analysis Framework, User's Guide
[9] S A Bass et al. 1998 *Prog. Part. Nucl. Phys.* **41** 225-370
[10] C Höhne et al. 2008 *J. Phys. G.* **35**, 104160